Am J Physiol Heart Circ Physiol
280: H1241–H1248, 2001.

Inflammatory pain alters blood-brain barrier permeability and tight junctional protein expression

J. D. HUBER, K. A. WITT, S. HOM, R. D. EGLETON, K. S. MARK, AND T. P. DAVIS
Department of Pharmacology, University of Arizona College of Medicine, Tucson, Arizona 85724

Received 27 July 2000; accepted in final form 23 October 2000

Huber, J. D., K. A. Witt, S. Hom, R. D. Egleton, K. S. Mark, and T. P. Davis. Inflammatory pain alters blood-brain barrier permeability and tight junctional protein expression. *Am J Physiol Heart Circ Physiol* 280: H1241–H1248, 2001.—Effects of inflammatory pain states on functional and molecular properties of the rat blood-brain barrier (BBB) were investigated. Inflammation was produced by subcutaneous injection of formalin, λ-carrageenan, or complete Freund's adjuvant (CFA) into the right hind paw. In situ perfusion and Western blot analyses were performed to assess BBB integrity after inflammatory insult. In situ brain perfusion determined that peripheral inflammation significantly increased the uptake of sucrose into the cerebral hemispheres. Capillary depletion and cerebral blood flow analyses indicated the perturbations were due to increased paracellular permeability rather than vascular volume changes. Western blot analyses showed altered tight junctional protein expression during peripheral inflammation. Occludin significantly decreased in the λ-carrageenan- and CFA-treated groups. Zonula occluden-1 expression was significantly increased in all pain models. Claudin-1 protein expression was present at the BBB and remained unchanged during inflammation. Actin expression was significantly increased in the λ-carrageenan- and CFA-treated groups. We have shown that inflammatory-mediated pain alters both the functional and molecular properties of the BBB. Inflammatory-induced changes may significantly alter delivery of therapeutic agents to the brain, thus affecting dosing regimens during chronic pain.

tight junctional proteins; microvascular endothelium; in situ perfusion; Western blot; cerebral blood flow

THE BLOOD-BRAIN BARRIER (BBB) is a physical and metabolic barrier between the central nervous system and the peripheral circulation that serves to regulate and protect the microenvironment of the brain. The BBB is characterized by the presence of tight junctions that result in a high transendothelial electrical resistance (1,500–2,000 Ω/cm^2) and a decrease in pinocytotic activity that restricts the diffusion of polar solutes across the endothelium (10). Several pathological states such as human immunodeficiency virus-1 encephalitis (13), multiple sclerosis (40), and hypoxia/aglycemia (1) induce altered permeability of the BBB. A breach in the BBB can lead to alterations in the central nervous system environment that effect ionic and nutritional balance and alter delivery of therapeutic agents. Larger BBB openings can result in increased serum protein uptake and edema (22).

Under basal physiological conditions, the brain microvessel endothelium acts as a barrier to the immune system limiting the entry of monocytes, lymphocytes, and other leukocytes (17, 31). However, proinflammatory mediators (i.e., cytokines, reactive oxygen species, and eicosanoids) can induce endothelial upregulation of specific surface adhesion molecules (such as platelet endothelial cell adhesion molecule-1, E-selectin, and intracellular adhesion molecule-1) and augment adhesion reactions and leukocyte migration (55). Several studies have reported a marked increase in membrane permeability after exposure to vasoactive substances such as tumor necrosis factor-α (20, 29), interleukin-1 (18), and histamine (25).

Although the research field is gaining insight into the molecular structure of tight junctions, much less is known about their regulation under physiological and pathophysiological conditions. Figure 1 illustrates the proposed interactions of the major proteins associated with tight junctions at the BBB. Tight junction strands are primarily composed of two distinct four transmembrane proteins, claudin and occludin. Claudins form dimers that bind homotypically to adjacent endothelial cells to form the primary seal of the tight junction (15). Claudins comprise a multigene family, and, to date, there are 20 claudin subtypes identified (50). Occludin, once believed to be the major tight junction protein, is found in high concentrations at BBB tight junctions (24); however, occludin is not necessary for tight junction formation (33). Rather, a previous study (6) has shown occludin presence increases electrical resistance across the junction.

Tight junctions also consist of several accessory proteins necessary to form structural support. The zonula occluden (ZO) proteins (ZO-1, ZO-2, and ZO-3) belong to the membrane-associated guanylate kinase-like proteins (MAGUKs), a family of proteins (21, 33) that serve as recognition proteins for tight junctional placement and support structures for signal transduction proteins (21).

Address for reprint requests and other correspondence: T. P. Davis, Dept. of Pharmacology, Univ. of Arizona College of Medicine, 1501 N. Campbell Ave., PO Box 24-5050, Tucson, AZ 85724-5050 (E-mail: davistp@u.arizona.edu).

The costs of publication of this article were defrayed in part by the payment of page charges. The article must therefore be hereby marked "*advertisement*" in accordance with 18 U.S.C. Section 1734 solely to indicate this fact.

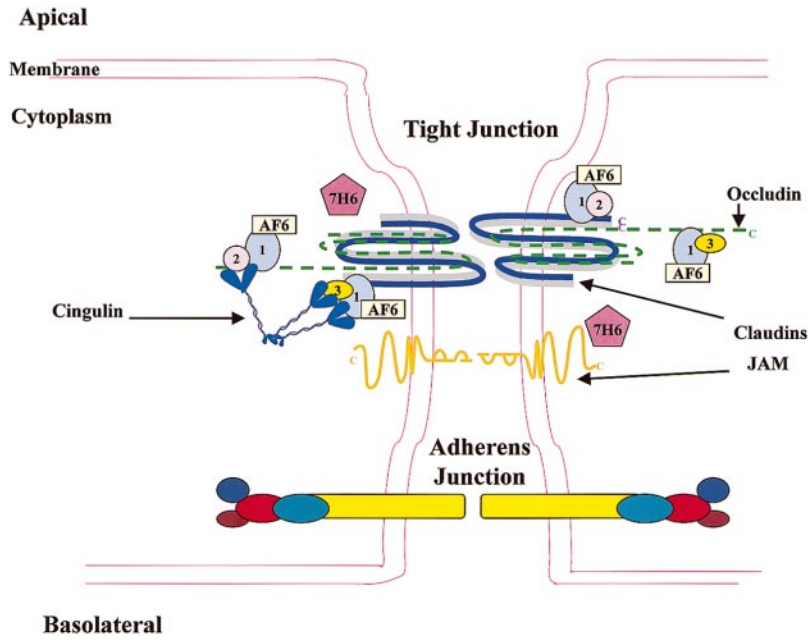

Fig. 1. Proposed interactions of the major proteins associated with tight junctions at the blood-brain barrier (BBB). Tight junctions consist of three integral protein types [claudins, occludins, and junctional adhesion molecules (JAM)]. Claudins form dimers with four transmembrane domains and bind homotypically to adjacent endothelial cells to form the primary seal of the tight junction (15). Occludin also has four transmembrane domains and is found in high concentrations at BBB tight junctions (24). JAM are localized at the tight junction and are members of the immunoglobin superfamily and may function in conjunction with platelet endothelial cell adhesion molecule-1 to regulate leukocyte migration (30). The tight junction also consists of several accessory proteins necessary to form structural support for the tight junction. The zonula occluden (ZO) proteins (ZO-1, ZO-2, and ZO-3) belong to a family of proteins known as membrane-associated guanylate kinase-like proteins (21, 33). These proteins serve as recognition proteins for tight junctional placement and as a support structure for signal transduction proteins (21). This diagram shows the known binding patterns for the ZO proteins to one another (54). AF6 is a Ras effector molecule associated with ZO-1 (27). The 7H6 antigen is a phosphoprotein found at tight junctions impermeable to ions and macromolecules (45). Cingulin is a double-stranded myosin-like protein that binds preferentially to ZO proteins at the globular head and to other cingulin molecules at the globular tail (12). The primary cytoskeletal protein actin has known binding sites on all of the ZO proteins, claudin, and occludin (26).

To date, little is known about peripheral inflammation influences on the BBB. In an effort to further understand the cellular mechanisms associated with inflammatory pain, we used three well-characterized and established inflammatory pain models in the rat. Inflammation was produced by unilateral subcutaneous injection of formalin, λ-carrageenan, or complete Freund's adjuvant (CFA) into the right hind paw. Each of these models is characterized by a different onset and time course of inflammatory response. With the use of this approach, we compared each pain model to determine whether peripheral inflammation has an effect on functional BBB permeability, cerebral blood flow (CBF), and expression of tight junctional proteins.

MATERIALS AND METHODS

Radioisotopes, antibodies, and chemicals. [^{14}C]sucrose was obtained from ICN Pharmaceuticals (specific activity, 492 mCi/mmol, >99.5% purity; Irvine, CA). *n*-[^{3}H]butanol was purchased from American Radiolabeled Chemicals (specific activity, 5 Ci/mmol, >99% purity; St. Louis, MO). Primary antibodies [anti-ZO-1 (1:1,500), anti-occludin (1:2,000), anti-actin (1:1,000), and anti-claudin-1 (1:1,500)] were obtained from Zymed (San Francisco, CA). Conjugated anti-rabbit IgG-horseradish peroxidase and anti-mouse IgG were purchased from Amersham (Springfield, IL). All other chemicals, unless otherwise stated, were purchased from Sigma (St. Louis, MO).

Animals and treatments. Female Sprague-Dawley rats (Harlan Sprague Dawley, Indianapolis, IN) weighing 250–300 g were housed under standard 12:12-h light-dark conditions and received food ad libitum. All protocols used in this study were approved by the University of Arizona Institutional Animal Care and Use Committee and abide by NIH guidelines. Rats were anesthetized with pentobarbital sodium (60 mg/kg ip) and subsequently injected (100 μl sc) with selected inflammatory agent into the plantar surface of the right hind paw. Pentobarbital sodium was used in this study to insure no interference with *N*-methyl-D-aspartate receptor activity. At 1-h postinjection, the 0.9% saline control and 5% formalin-injected rats underwent a 20-min in situ perfusion, or the brain was harvested for Western blot analyses. λ-Carrageenan (3%)- and CFA (50%)-injected rats underwent the same procedures at 3 h and 3 days, respectively.

In situ brain perfusion. Rats were anesthetized as above and heparinized (10,000 U/kg). Body temperature was maintained using a heating pad. The ipsilateral common carotid artery was exposed and cannulated with silicone tubing connected to a perfusion circuit. The perfusate consisted of a modified mammalian Ringer solution consisting of (in mM) 117 NaCl, 4.7 KCl, 0.8 $MgSO_4$, 24.8 $NaHCO_3$, 1.2 KH_2PO_4, 2.5 $CaCl_2$, and 10 D-glucose and 3.9% dextran (molecular weight 70,000) and 1 g/l bovine serum albumin (type V) (38).

The addition of Evans blue (55 mg/l) to the Ringer solution provided a control for BBB integrity. The perfusate was aerated with 95% O_2-5% CO_2 and warmed to 37°C. The ipsilateral vein was sectioned to allow drainage. Once the desired perfusion pressure and flow rate were achieved (85–95 mmHg and 3.1 ml/min, respectively), the contralateral carotid artery was cannulated and perfused as described above. Radiolabeled sucrose was infused using a slow-drive syringe pump (0.5 ml/min per hemisphere; model 22, Harvard Apparatus, South Natick, MA) into the inflow of the perfusate. The animal was decapitated, and the brain was removed. The choroid plexus and meninges were excised, and the cerebral hemispheres were sectioned and homogenized. Perfusate containing the radiolabeled marker was collected from each carotid cannula at the termination of the perfusion to serve as a reference.

Cerebral hemispheres (~500 mg) and 100 μl of perfusate were prepared for liquid scintillation counting by adding 1 ml of tissue solubilizer (TS-2; Research Products, Mount Pleasant, IL). After 2 days of solubilization, 100 μl of 30% glacial acetic acid was added to eliminate chemiluminescence. Budget Solve Liquid Scintillation Cocktail (4 ml) (Research Products) was added, and samples were measured for radioactivity (model LS 5000 TD Counter; Beckman Instruments, Fullerton, CA).

Capillary depletion. Measurement of the vascular component to total brain uptake was performed using capillary depletion (49, 58). After a 20-min in situ perfusion, the brain was removed, and the choroid plexus and meninges were excised. The brain tissue (50 mg wet wt) was homogenized (Polytron homogenizer, Brinkman Instruments, Westbury NY) in 1.5 ml of capillary depletion buffer [containing (in mM) 10 4-(2-hydroxyethyl)-piperaxineethane sulfonic acid, 141 NaCl, 4 KCl, 2.8 $CaCl_2$, 1 $MgSO_4$, 1 NaH_2PO_4, and 10 D-glucose; pH 7.4] and kept on ice. Ice-cold 26% clinical grade dextran (2 ml) was added, and the homogenization was repeated. Aliquots of homogenate were centrifuged at 5,400 *g* for 15 min in a microfuge (Beckman Instruments). Capillary-depleted supernatant was separated from the vascular pellet. All of the homogenization procedures were performed within 2 min of euthanizing the animal. The homogenate, supernatant, and pellet were taken for radioactive counting. The amount of [^{14}C]sucrose in the brain homogenate, supernatant, and pellet (C_{tissue}; in disintegrations·min^{-1}·g^{-1} of disintergrations·min^{-1}·ml^{-1}) to the amount of [^{14}C]sucrose in the perfusate ($C_{perfusate}$; in disintegrations·min^{-1}·ml^{-1}) was expressed as the ratio of tissue to perfusate activities (R_{tissue})

$$R_{tissue} = (C_{tissue}/C_{perfusate}) \times 100\% \quad (1)$$

Cerebral blood flow. The perfusion method of Preston et al. (38) and Zlokovic et al. (59) was adapted to determine both CBF and the rate of cerebral perfusion in situ using the derived equations of Gjedde et al. (16) for [^{3}H]butanol uptake. In situ brain perfusion was carried out as stated above with a Ringers solution containing 4 ml/l unlabeled ethanol. With the use of a slow-drive syringe pump (0.5 ml/min per hemisphere), [^{3}H]butanol was added during last 10 s of a 20-min perfusion. A partition coefficient (λ_{br}) was determined using a separate group of animals perfused with a constant [^{3}H]butanol concentration in the arterial inflow for 20 min followed by brain sampling and analysis. Brains were immediately weighed and sectioned. Brain and Ringer solution samples were taken for liquid scintillation counting. A small portion of the frontal lobes (~50 mg) was removed and weighed separately to determine the brain tissue dry weight by drying in an oven at 95°C to constant weight. Unlabeled ethanol was added to saturate endogenous alcohol dehydrogenase for both measurements.

Calculation of CBF. The basic treatment of Gjedde et al. (16) was followed using the derived equation

$$F_{bl} = -\lambda_{br} \ln[(1 - C_{br(t)}/\lambda_{br} \times C_a)/t] \quad (2)$$

where F_{bl} is the rate of blood flow [in ml/min per unit mass (g)] and C_a is the constant [^{3}H]butanol concentration in arterial inflow at *time t* between the introduction of [^{3}H]butanol and decapitation. C_{br} is the activity in unit weight of brain at *time t*. λ_{br} is the distribution ratio of [^{3}H]butanol between the brain and the perfusion medium at the steady state. The value of λ_{br} was calculated as the ratio of the ^{3}H radioactivity in the brain versus ^{3}H radioactivity in the arterial inflow. Extraction of the tracer from the blood is assumed to be complete during a single capillary pass.

Tight junctional protein analysis. After capillary depletion and protein extraction, microvasculature samples (20 μg) were resolved on a 4–12% Tris-glycine gel (Novex, San Diego, CA) for 90 min at 125 V and transferred to a polyvinylidene difluoride membrane for 40 min at 240 mA. Polyvinylidene difluoride membranes were blocked in Tris-buffered saline (141 mM NaCl, 10 mM Tris-base, and 0.1% Tween 20) with 5% nonfat milk for 4 h. Blots were incubated with primary antibody at room temperature for 2 h, rinsed with Tris-buffered saline with 5% nonfat milk for 1 h, and incubated with secondary antibody for 1 h. Blots were developed using enhanced chemiluminescence (ECL+, Amersham, Springfield, IL) and analyzed using Scion image software.

RESULTS

In situ brain perfusion. The effect of inflammation on basal permeability across an intact BBB was assessed

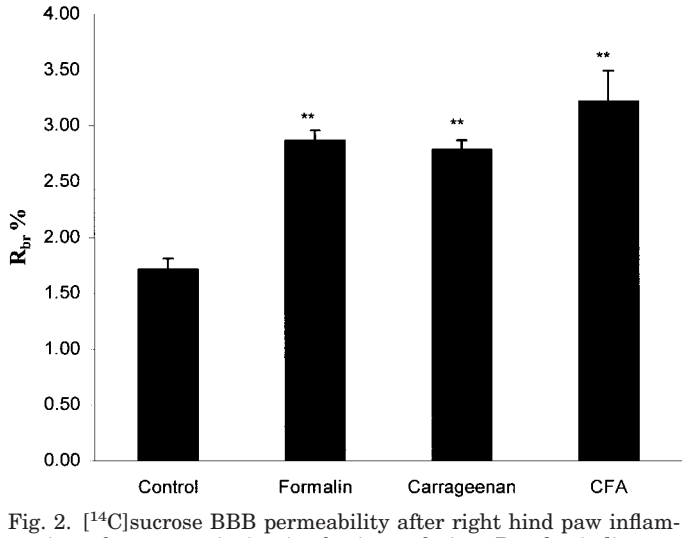

Fig. 2. [^{14}C]sucrose BBB permeability after right hind paw inflammation after a 20-min in situ brain perfusion. Results indicate a significantly higher distribution of sucrose in the cerebral hemispheres for all inflammatory pain models [formalin, 67.3%; λ-carrageenan, 62.5%; and complete Freund's adjuvant (CFA), 87.6%] compared with that in control. R_{br}, ratio of radioactivity found in the brain compared with the radioactivity found in the perfusate media. Each bar represents the mean ± SE (n = 7–8). Statistical significance was determined using one-way ANOVA followed by Newman-Keuls post hoc test. $^{**}P < 0.01$ vs. control.

Table 1. *Capillary depletion studies after a 20-min in situ perfusion*

Capillary Depletion Data	Pellet	Supernatant	Homogenate
Control	0.690 ± 0.168†	1.709 ± 0.086	1.860 ± 0.108
Formalin	0.794 ± 0.169†	1.935 ± 0.102	2.309 ± 0.115*
λ-Carrageenan	0.920 ± 0.149†	2.479 ± 0.175*	2.919 ± 0.167*
CFA	1.161 ± 0.247†	3.191 ± 0.301*	3.129 ± 0.141*

Values are means ± SE; $n = 4$. Data are the percent values after a 20-min in situ perfusion with [^{14}C]sucrose. CFA, complete Freund's adjuvant. Statistical significance was determined using 2-way ANOVA. *$P < 0.01$, significant difference from control within group (pellet, supernatant, or homogenate); †$P < 0.01$, significant difference from homogenate.

using in situ perfusion of the brain with [^{14}C]sucrose, a membrane-impermeant marker. Visual inspection of the brain immediately after in situ perfusion showed no influx of Evans blue albumin into the brain parenchyma.

Figure 2 shows the control group, representing the vascular space volume, and the three inflammatory pain models. The control ratio of the radioactivity found in the brain to radioactivity found in the perfusate media (R_{br}) value of 1.71 ± 0.09% was converted to a vascular space of 17.1 μl/g brain tissue. The results indicate a significantly ($P < 0.01$) higher distribution of sucrose into the brain in all three inflammatory pain models (formalin, 67.3%; λ-carrageenan, 62.5%; and CFA, 87.6%) compared with control.

Capillary depletion. Table 1 shows capillary depletion data after a 20-min in situ perfusion. Capillary depletion showed the amount of [^{14}C]sucrose trapped in the pellet of all three treatment groups was not significantly different from that in control. Furthermore, the study revealed that the percent amount of [^{14}C]sucrose associated with actual entry into the brain parenchyma (supernatant) was not statistically different from that in the homogenate.

Cerebral blood flow. Table 2 shows parameters measured for CBF after a 20-min in situ perfusion. The cerebral perfusion pressures and rates showed no difference among the three pain models compared with control. CBF (F_{bl}) was calculated at $t = 10$ s: $C_{br(t)}$ = control, 0.76 ± 0.07 μCi/g; formalin, 0.98 ± 0.12 μCi/g; λ-carrageenan, 1.16 ± 0.20 μCi/g; and CFA, 1.07 ± 0.20 μCi/g; C_a = control, 34.11 ± 0.75 nCi/g; formalin, 33.07 ± 1.88 nCi/g; λ-carrageenan, 38.06 ± 1.05 nCi/g; and CFA, 37.62 ± 1.77 nCi/g; and λ_{br} = control, 0.61; formalin, 0.64; λ-carrageenan, 0.80; and CFA, 0.52. The results showed a significant ($P < 0.01$) increase in CBF in all inflammatory pain models (Table 2) compared with CBF in control (0.82 ± 0.01 ml·min^{-1}·g^{-1}). Brain weights and the percent water content were similar among all treatment groups compared with control.

Tight junctional protein analysis. Western blot analyses indicate that the expression of tight junction proteins can be altered during peripheral inflammation. Figure 3*A* shows that the integral protein occludin was significantly decreased in the λ-carrageenan and CFA treatment groups (56.9 ± 13.6 and 26.9 ± 10.8% of control, respectively). Figure 3*B* illustrates a significant ($P < 0.01$) increase in ZO-1 protein expression in all three inflammation groups compared with control (formalin, 158.9 ± 1.9%; λ-carrageenan, 239.3 ± 8.3%; and CFA, 187.1 ± 4.4%). Figure 3*C* shows no significant difference in actin expression between the formalin and control groups; however, there is a significant ($P < 0.01$) increase in actin expression in both the λ-carrageenan and CFA groups compared with control (299.5 ± 38.4 and 261.7 ± 29.7%, respectively). Figure 3*D* illustrates that claudin-1 is present in the rat microvascular endothelium and that claudin-1 expression was unchanged in all inflammatory pain models compared with control.

DISCUSSION

In this study, three different inflammatory pain models (acute, short term, and long term) were used to examine in vivo BBB permeability effects after peripheral inflammation stimuli. The effect of inflammation on basal permeability across an intact BBB was assessed using in situ brain perfusion with [^{14}C]sucrose. The control R_{br} value of 1.71% was converted to a vascular space of 17.1 μl/g brain tissue, which is similar to that found in other studies (7, 23, 53) using vascular markers (3–20 μl/g brain). Each of the three inflammatory pain models produced significant increases in R_{br}, indicating either a change in vascular volume and/or an increased BBB permeability (Fig. 2).

To investigate this finding further, capillary depletion and CBF studies were performed to insure that the increased BBB permeabilities were due to increased paracellular diffusion and not changes in vascular space or vascular trapping. Capillary depletion

Table 2. *Cerebral blood flow analyses after a 20-min in situ perfusion*

Treatment	Control	Formalin	λ-Carrageenan	CFA
λ_{br}	0.61 ± 0.06(3)	0.64 ± 0.05(3)	0.80 ± 0.10(3)	0.59 ± 0.05(3)
Perfusion pressure, mmHg	93.61 ± 3.55(9)	83.68 ± 3.49(8)	80.15 ± 3.59(8)	82.98 ± 3.11(8)
Perfusion rate, ml·min^{-1}·g^{-1}	1.70 ± 0.019(5)	1.66 ± 0.042(4)	1.71 ± 0.015(4)	1.72 ± 0.007(4)
Cerebral blood flow, ml·min^{-1}·g^{-1}	0.82 ± 0.01(5)	0.94 ± 0.01†(4)	1.41 ± 0.03†(4)	0.89 ± 0.02*(4)
Perfused brain weight, g	1.82 ± 0.02(5)	1.87 ± 0.046(5)	1.81 ± 0.016(5)	1.80 ± 0.008(5)
Perfused brain water, %	82.65 ± 0.11(5)	82.57 ± 1.14(5)	82.108 ± 0.72(5)	84.47 ± 1.00(5)

Values are means ± SE; numbers in parentheses are numbers of rats. λ_{br}, Distribution ratio of [^{3}H]butanol between the brain and perfusion medium at the steady state. Significance was determined using one-way ANOVA followed by a Newman-Keuls post hoc test. *$P < 0.05$, †$P < 0.01$ vs. control.

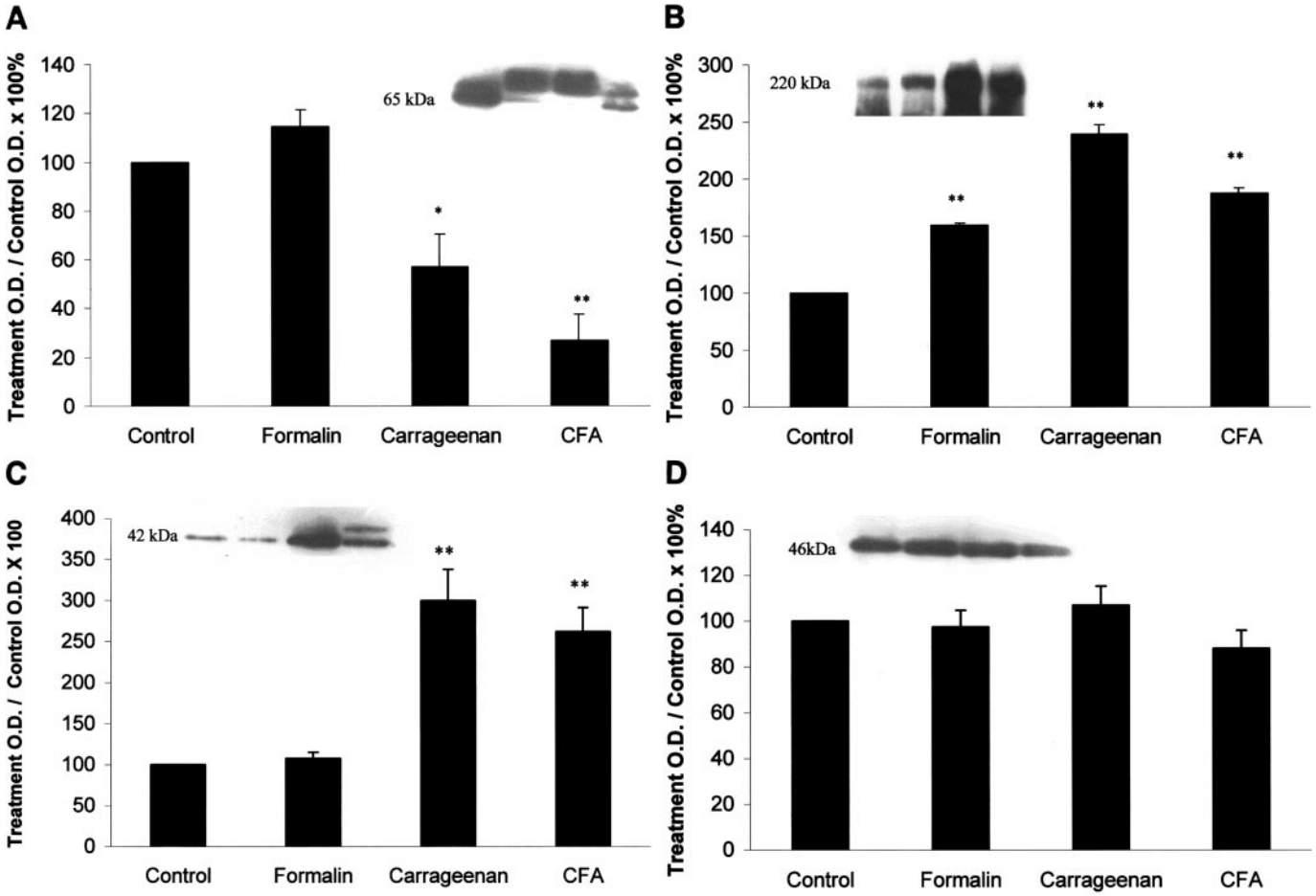

Fig. 3. Western blot analyses indicate that expression of tight junctional proteins can be altered during peripheral inflammation. *A*: the integral protein occludin was significantly decreased in the λ-carrageenan and CFA inflammatory pain models (56.9 ± 13.6 and 26.9 ± 10.8% of control, respectively). *B*: ZO-1 expression was significantly increased in all 3 inflammatory pain models compared with control (formalin, 158.9 ± 1.9%; λ-carrageenan, 239.3 ± 8.3%; and CFA, 187.1 ± 4.4%). *C*: no differences were seen in actin expression between the formalin and control groups; however, there was a significant difference in actin expression in both the λ-carrageenan and CFA inflammatory pain models compared with that in control (299.5 ± 38.4 and 261.7 ± 29.7%, respectively). *D*: claudin-1 expression was unchanged in the 3 inflammation groups compared with the control. Each bar represents the mean ± SE (n = 3 rats/group). *Insets*: representative Western blots. *Lane 1*, control; *lane 2*, formalin; *lane 3*, λ-carrageenan; *lane 4*, CFA. Statistical significance was determined using one-way ANOVA followed by Newman-Keuls post hoc test. *$P < 0.05$, **$P < 0.01$ vs. control.

studies (Table 1) showed the amount of sucrose trapped in the vascular pellet of each of the three pain models was not statistically different from control. Furthermore, the increased sucrose associated with the supernatant in the λ-carrageenan and CFA groups indicates a breach in the BBB.

CBF measured in control rats (0.82 ± 0.01 $ml \cdot min^{-1} \cdot g^{-1}$) using [^{3}H]butanol was consistent with previously reported values ranging from 0.8–1.49 $ml \cdot min^{-1} \cdot g^{-1}$ (16, 42). In addition, a recent study (57) using magnetic resonance imaging determined the in vivo CBF in rats to be 1.29 ± 0.44 $ml \cdot min^{-1} \cdot g^{-1}$. The current study showed a significant ($P < 0.01$) increase in CBF with all three inflammatory pain models (Table 2). These CBF increases corresponded with the nonsignificant increase in pellet sucrose found after capillary depletion (Table 1) and suggest a slight increase in vascular volume. Cerebral autoregulation protects the brain from fluctuations in pressure and flow in the peripheral circulation to maintain a constant perfusion of the brain; therefore, cerebral flow dynamics must be taken into account to insure no alterations in perfusion have occurred. In the present study, the increases in CBF were paralleled by only a small drop in perfusion pressure and a constant perfusion rate, indicating cerebral autoregulation was maintained during inflammation. In addition, the unchanged percentages of brain water suggest that edema formation was negligible. These studies clearly indicate that inflammatory pain produced significant increases in BBB permeability via increased paracellular diffusion between the brain microvascular endothelium.

Western blot analyses were performed to determine whether the perturbations seen in BBB permeability were associated with alterations in tight junctions. Although the research field is gaining insight into the

molecular structure of endothelial cell tight junctions, much less is known about their regulation under physiological (Fig. 1) and pathophysiological conditions. Tight junction assembly and function can be modulated by a number of signaling molecules, including cAMP, Ca^{2+}, G proteins, phospholipase C, diacylglycerol, small GTP-binding proteins, and protein kinase C (5, 19, 28, 36, 43). Although occludin is not necessary for tight junction formation (33), a previous study (6) has shown that the presence of occludin increases electrical resistance across the junction. Previously, it was reported that interleukin-1β decreased occludin expression and increased BBB permeability (9). Similarly, the current study showed a dramatic decrease in the expression of occludin in the λ-carrageenan (3 h) and CFA (3 days) groups (Fig. 3*A*).

Under physiological conditions, phosphorylation regulates the maintenance and assembly of tight junctions (37, 44, 56). Occludin can be phosphorylated on serine, threonine, and tyrosine residues (44, 47, 48). Excessive tyrosine phosphorylation has been shown to increase transcellular permeability in epithelial and endothelial cells (18, 48). Wachtel et al. (52) reported that tyrosine phosphatase inhibition led to occludin proteolysis and increased tight junctional permeability in human umbilical vein endothelial cells. Furthermore, studies (2, 3) involving diabetic retinopathy have shown that vascular endothelial growth factor stimulated rapid tyrosine phosphorylation of occludin and ZO-1 that led to a 35% decrease in occludin and increased vascular permeability. As a result, excessive or unregulated phosphorylation, especially on tyrosine residues, appears to increase BBB permeability due to a decreased expression of occludin at the tight junction. Thus occludin expression is an important determinant in assessing paracellular permeability of tight junctions, and decreases in occludin expression may be due to an inflammation-induced increase in tyrosine phosphorylation. A possible contributing factor to the susceptibility of occludin to tyrosine phosphorylation is the high concentration of glycine and tyrosine (~65%) in the first extracellular loop (14). Further studies are necessary to investigate the phosphorylation patterns and time course of occludin loss during inflammation.

ZO-1, a structural protein important in forming tight junctional cytoplasmic plaques (46), also has phosphorylation sites on serine, threonine, and tyrosine residues (4, 11, 47, 48). Unlike occludin, excessive phosphorylation of ZO-1 has not been shown to decrease expression (52). Rather, ZO-1 has shown variability in actions after increased phosphorylation. In Madin Darby canine kidney cells, protein phosphatase inhibitors increased tyrosine phosphorylation of several junctional proteins, including ZO-1, with a concomitant decrease in transepithelial electrical resistance (39). In subconfluent human epidermoid carcinoma cells (A431), epithelial growth factor stimulation of ZO-1 tyrosine phosphorylation was associated with movement from a diffuse cytoplasmic location to the plasma membrane (51). In this study, an increased expression of ZO-1 was observed in both short-term and long-term inflammatory models [λ-carrageenan (3 h) and CFA (3 days)] (Fig. 2*B*). This increase in expression may be due to a transcriptional increase in ZO-1; however, a more probable explanation is that the change in expression is due to a change in phosphorylation states. The change in phosphorylation of ZO-1 is likely to be a compensatory mechanism by the cell to recruit more tight junctional proteins from the cytoplasm to the plasma membrane.

ZO-1 and actin showed increased trends in expression after peripheral inflammation (Fig. 2*C*). These similarities may be due to the tight association of ZO-1 with actin filaments. A previous study (8) has shown reorganization of the cytoskeletal architecture after pathological insult. The increased expression of actin, in conjunction with its high association with ZO-1, suggests a reorganization of the cytoskeleton to maintain BBB tight junctional integrity.

Claudin proteins embed in the plasma membrane as dimerized strands, which interact with the claudins of adjacent cells to form a seal (15). The impermeability of the tight junction is related to the strength of the interactions between claudin strands and varies dependently on the claudin species involved and their combinations (15). Immunoflourescence studies (32, 34) in mice have shown that claudin-4 and -8 comprise the tight junctions of the kidney, claudin-1, -2, and -3 are found in the liver, and claudin-11 composes the tight junction of the Sertoli cells in the testis. To date, claudin variants responsible for the tight junctions of the BBB are unknown. Endothelial cells forming the BBB are coupled by tight junctions of extremely low permeability that resemble those of epithelial barriers (41). A recent study (35) has shown that claudin-2, -3, -4, -8, -11, and -14 were not detected in endothelial cells and that claudin-5 was not expressed in capillary endothelial cells. Thus studies need to be performed on the remaining claudin subtypes to determine their presence and roles in BBB tight junctions.

In this study, we examined the expression of claudin-1 and determined its presence in the capillaries of the BBB (Fig. 2*D*). This study is one of the first to identify a claudin subtype in the brain microvasculature of the rat. Claudin-1 expression was located at 46 kDa, indicating its presence in the dimerized form. The unchanged expression of claudin-1 after inflammation suggests that BBB tight junctions remained intact during inflammation. This finding supports a previous study (15) suggesting that claudin is the major protein involved in maintaining tight junctional integrity.

We have shown that inflammatory-mediated pain states alter both the functional and molecular properties of the BBB. In fact, we demonstrate a correlation between increased BBB permeability and altered expression of important tight junctional proteins. These results suggest that peripheral inflammation stimulates reorganization of tight junctions, leading to increased paracellular diffusion. While occludin and ZO-1 play critical roles in regulating permeability changes at the tight junctions, the exact mechanism(s) remains unclear. Previous reports suggest that these

proteins are regulated by their phosphorylation states and play an important role in how tight junctions alter permeability during various immune-mediated pain states. This is the first report of peripheral inflammation inducing alterations in tight junctions and increasing permeability of the BBB. These inflammatory-mediated BBB changes may have a significant impact on the delivery of therapeutic agents to the brain. Clinical dosing regimens during chronic inflammatory pain will need to be reevaluated in light of these new findings.

This study was funded by National Institutes of Health Grants DA-11271, NS-39592, and DA-06037.

REFERENCES

1. **Abbruscato TJ and Davis TP.** Combination of hypoxia/aglycemia compromises in vitro blood-brain barrier integrity. *J Pharmacol Exp Ther* 289: 668–675, 1999.
2. **Antonetti DA, Barber AJ, Khin S, Lieth E, Tarbell JM, and Gardner TW.** Vascular permeability in experimental diabetes is associated with reduced endothelial occludin content: vascular endothelial growth factor decreases occludin in retinal endothelial cells. Penn State Retina Research Group. *Diabetes* 47: 1953–1959, 1998.
3. **Antonetti DA, Lieth E, Barber AJ, and Gardner TW.** Molecular mechanisms of vascular permeability in diabetic retinopathy. *Semin Ophthalmol* 14: 240–248, 1999.
4. **Balda MS, Anderson JM, and Matter K.** The SH3 domain of the tight junction protein ZO-1 binds to a serine protein kinase that phosphorylates a region C-terminal to this domain. *FEBS Lett* 399: 326–332, 1996.
5. **Balda MS, Gonzalez-Mariscal L, Matter K, Cereijido M, and Anderson JM.** Assembly of the tight junction: the role of diacylglycerol. *J Cell Biol* 123: 293–302, 1993.
6. **Balda MS, Whitney JA, Flores C, Gonzalez S, Cereijido M, and Matter K.** Functional dissociation of paracellular permeability and transepithelial electrical resistance and disruption of the apical-basolateral intramembrane diffusion barrier by expression of a mutant tight junction membrane protein. *J Cell Biol* 134: 1031–1049, 1996.
7. **Blasberg RG, Patlak CS, and Fenstermacher JD.** Selection of experimental conditions for the accurate determination of blood-brain transfer constants from single-time experiments: a theoretical analysis. *J Cereb Blood Flow Metab* 3: 215–225, 1983.
8. **Blum MS, Toninelli E, Anderson JM, Balda MS, Zhou J, O'Donnell L, Pardi R, and Bender JR.** Cytoskeletal rearrangement mediates human microvascular endothelial tight junction modulation by cytokines. *Am J Physiol Heart Circ Physiol* 273: H286–H294, 1997.
9. **Bolton SJ, Anthony DC, and Perry VH.** Loss of the tight junction proteins occludin and zonula occludens-1 from cerebral vascular endothelium during neutrophil-induced blood-brain barrier breakdown in vivo. *Neuroscience* 86: 1245–1257, 1998.
10. **Butt AM, Jones HC, and Abbott NJ.** Electrical resistance across the blood-brain barrier in anaesthetized rats: a developmental study. *J Physiol (Lond)* 429: 47–62, 1990.
11. **Collares-Buzato CB, Jepson MA, Simmons NL, and Hirst BH.** Increased tyrosine phosphorylation causes redistribution of adherens junction and tight junction proteins and perturbs paracellular barrier function in MDCK epithelia. *Eur J Cell Biol* 76: 85–92, 1998.
12. **Cordenonsi M, D'Atri F, Hammar E, Parry DA, Kendrick-Jones J, Shore D, and Citi S.** Cingulin contains globular and coiled-coil domains and interacts with ZO-1, ZO-2, ZO-3, and myosin. *J Cell Biol* 147: 1569–1582, 1999.
13. **Dallasta LM, Pisarov LA, Esplen JE, Werley JV, Moses AV, Nelson JA, and Achim CL.** Blood-brain barrier tight junction disruption in human immunodeficiency virus-1 encephalitis. *Am J Pathol* 155: 1915–1927, 1999.
14. **Furuse M, Itoh M, Hirase T, Nagafuchi A, Yonemura S, and Tsukita S.** Direct association of occludin with ZO-1 and its possible involvement in the localization of occludin at tight junctions. *J Cell Biol* 127: 1617–1626, 1994.
15. **Furuse M, Sasaki H, and Tsukita S.** Manner of interaction of heterogeneous claudin species within and between tight junction strands. *J Cell Biol* 147: 891–903, 1999.
16. **Gjedde A, Hansen AJ, and Siemkowicz E.** Rapid simultaneous determination of regional blood flow and blood-brain glucose transfer in brain of rat. *Acta Physiol Scand* 108: 321–330, 1980.
17. **Glabinski AR.** Chemokines in central nervous system pathology. *Neurol Neurochir Pol* 33: 897–906, 1999.
18. **Gloor SM, Weber A, Adachi N, and Frei K.** Interleukin-1 modulates protein tyrosine phosphatase activity and permeability of brain endothelial cells. *Biochem Biophys Res Commun* 239: 804–809, 1997.
19. **Gonzalez-Mariscal L, Chavez de Ramirez B, and Cereijido M.** Tight junction formation in cultured epithelial cells (MDCK). *J Membr Biol* 86: 113–125, 1985.
20. **Guo YL, Kang B, and Williamson JR.** Resistance to TNF-α cytotoxicity can be achieved through different signaling pathways in rat mesangial cells. *Am J Physiol Cell Physiol* 276: C435–C441, 1999.
21. **Haskins J, Gu L, Wittchen ES, Hibbard J, and Stevenson BR.** ZO-3, a novel member of the MAGUK protein family found at the tight junction, interacts with ZO-1 and occludin. *J Cell Biol* 141: 199–208, 1998.
22. **Hatashita S and Hoff JT.** Brain edema and cerebrovascular permeability during cerebral ischemia in rats. *Stroke* 21: 582–588, 1990.
23. **Heisey SR.** Brain and choroid plexus blood volumes in vertebrates. *Comp Biochem Physiol* 26: 489–498, 1968.
24. **Hirase T, Staddon JM, Saitou M, Ando-Akatsuka Y, Itoh M, Furuse M, Fujimoto K, Tsukita S, and Rubin LL.** Occludin as a possible determinant of tight junction permeability in endothelial cells. *J Cell Sci* 110: 1603–1613, 1997.
25. **Hurst RD and Clark JB.** Alterations in transendothelial electrical resistance by vasoactive agonists and cyclic AMP in a blood-brain barrier model system. *Neurochem Res* 23: 149–154, 1998.
26. **Itoh M, Furuse M, Morita K, Kubota K, Saitou M, and Tsukita S.** Direct binding of three tight junction-associated MAGUKs, ZO-1, ZO-2, and ZO-3, with the COOH termini of claudins. *J Cell Biol* 147: 1351–1363, 1999.
27. **Joh T, Yamamoto K, Kagami Y, Kakuda H, Sato T, Yamamoto T, Takahashi T, Ueda R, Kaibuchi K, and Seto M.** Chimeric MLL products with a Ras binding cytoplasmic protein AF6 involved in t(6;11) (q27;q23) leukemia localize in the nucleus. *Oncogene* 15: 1681–1687, 1997.
28. **Jou TS, Schneeberger EE, and Nelson WJ.** Structural and functional regulation of tight junctions by RhoA and Rac1 small GTPases. *J Cell Biol* 142: 101–115, 1998.
29. **Mark KS and Miller DW.** Increased permeability of primary cultured brain microvessel endothelial cell monolayers following TNF-alpha exposure. *Life Sci* 64: 1941–1953, 1999.
30. **Martin-Padura I, Lostaglio S, Schneemann M, Williams L, Romano M, Fruscella P, Panzeri C, Stoppacciaro A, Ruco L, Villa A, Simmons D, and Dejana E.** Junctional adhesion molecule, a novel member of the immunoglobulin superfamily that distributes at intercellular junctions and modulates monocyte transmigration. *J Cell Biol* 142: 117–127, 1998.
31. **Miller DW.** Immunobiology of the blood-brain barrier. *J Neurovirol* 5: 570–578, 1999.
32. **Morita K, Furuse M, Fujimoto K, and Tsukita S.** Claudin multigene family encoding four-transmembrane domain protein components of tight junction strands. *Proc Natl Acad Sci USA* 96: 511–516, 1999.
33. **Morita K, Itoh M, Saitou M, Ando-Akatsuka Y, Furuse M, Yoneda K, Imamura S, Fujimoto K, and Tsukita S.** Subcellular distribution of tight junction-associated proteins (occludin, ZO-1, ZO-2) in rodent skin. *J Invest Dermatol* 110: 862–866, 1998.

34. **Morita K, Sasaki H, Fujimoto K, Furuse M, and Tsukita S.** Claudin-11/OSP-based tight junctions of myelin sheaths in brain and Sertoli cells in testis. *J Cell Biol* 145: 579–588, 1999.
35. **Morita K, Sasaki H, Furuse M, and Tsukita S.** Endothelial claudin: claudin-5/TMVCF constitutes tight junction strands in endothelial cells. *J Cell Biol* 147: 185–194, 1999.
36. **Mullin JM, Kampherstein JA, Laughlin KV, Clarkin CE, Miller RD, Szallasi Z, Kachar B, Soler AP, and Rosson D.** Overexpression of protein kinase C-δ increases tight junction permeability in LLC-PK1 epithelia. *Am J Physiol Cell Physiol* 275: C544–C554, 1998.
37. **Nigam SK, Denisenko N, Rodriguez-Boulan E, and Citi S.** The role of phosphorylation in development of tight junctions in cultured renal epithelial (MDCK) cells. *Biochem Biophys Res Commun* 181: 548–553, 1991.
38. **Preston JE, al-Sarraf H, and Segal MB.** Permeability of the developing blood-brain barrier to ^{14}C-mannitol using the rat in situ brain perfusion technique. *Brain Res Dev Brain Res* 87: 69–76, 1995.
39. **Ratcliffe MJ, Smales C, and Staddon JM.** Dephosphorylation of the catenins p120 and p100 in endothelial cells in response to inflammatory stimuli. *Biochem J* 338: 471–478, 1999.
40. **Rousseau V, Denizot B, Le Jeune JJ, and Jallet P.** Early detection of liposome brain localization in rat experimental allergic encephalomyelitis. *Exp Brain Res* 125: 255–264, 1999.
41. **Rubin LL.** Endothelial cells: adhesion and tight junctions. *Curr Opin Cell Biol* 4: 830–833, 1992.
42. **Sage JI, Van Uitert RL, and Duffy TE.** Simultaneous measurement of cerebral blood flow and unidirectional movement of substances across the blood-brain barrier: theory, method, and application to leucine. *J Neurochem* 36: 1731–1738, 1981.
43. **Saha C, Nigam SK, and Denker BM.** Involvement of Galphai2 in the maintenance and biogenesis of epithelial cell tight junctions. *J Biol Chem* 273: 21629–21633, 1998.
44. **Sakakibara A, Furuse M, Saitou M, Ando-Akatsuka Y, and Tsukita S.** Possible involvement of phosphorylation of occludin in tight junction formation. *J Cell Biol* 137: 1393–1401, 1997.
45. **Satoh H, Zhong Y, Isomura H, Saitoh M, Enomoto K, Sawada N, and Mori M.** Localization of 7H6 tight junction-associated antigen along the cell border of vascular endothelial cells correlates with paracellular barrier function against ions, large molecules, and cancer cells. *Exp Cell Res* 222: 269–274, 1996.
46. **Sheth B, Fesenko I, Collins JE, Moran B, Wild AE, Anderson JM, and Fleming TP.** Tight junction assembly during mouse blastocyst formation is regulated by late expression of ZO-1 alpha+ isoform. *Development* 124: 2027–20237, 1997.
47. **Singer KL, Stevenson BR, Woo PL, and Firestone GL.** Relationship of serine/threonine phosphorylation/dephosphorylation signaling to glucocorticoid regulation of tight junction permeability and ZO-1 distribution in nontransformed mammary epithelial cells. *J Biol Chem* 269: 16108–16115, 1994.
48. **Staddon JM, Herrenknecht K, Smales C, and Rubin LL.** Evidence that tyrosine phosphorylation may increase tight junction permeability. *J Cell Sci* 108: 609–619, 1995.
49. **Triguero D, Buciak J, and Pardridge WM.** Capillary depletion method for quantification of blood-brain barrier transport of circulating peptides and plasma proteins. *J Neurochem* 54: 1882–1888, 1990.
50. **Tsukita S and Furuse M.** Pores in the wall: claudins constitute tight junction strands containing aqueous pores. *J Cell Biol* 149: 13–16, 2000.
51. **Van Itallie CM, Balda MS, and Anderson JM.** Epidermal growth factor induces tyrosine phosphorylation and reorganization of the tight junction protein ZO-1 in A431 cells. *J Cell Sci* 108: 1735–1742, 1995.
52. **Wachtel M, Frei K, Ehler E, Fontana A, Winterhalter K, and Gloor SM.** Occludin proteolysis and increased permeability in endothelial cells through tyrosine phosphatase inhibition. *J Cell Sci* 112: 4347–4356, 1999.
53. **Williams SA, Abbruscato TJ, Hruby VJ, and Davis TP.** Passage of a delta-opioid receptor selective enkephalin, [D-penicillamine-2,5] enkephalin, across the blood-brain and the blood- cerebrospinal fluid barriers. *J Neurochem* 66: 1289–1299, 1996.
54. **Wittchen ES, Haskins J, and Stevenson BR.** Protein interactions at the tight junction. Actin has multiple binding partners, and ZO-1 forms independent complexes with ZO-2 and ZO-3. *J Biol Chem* 274: 35179–35185, 1999.
55. **Wong D, Prameya R, and Dorovini-Zis K.** In vitro adhesion and migration of T lymphocytes across monolayers of human brain microvessel endothelial cells: regulation by ICAM-1, VCAM- 1, E-selectin and PECAM-1. *J Neuropathol Exp Neurol* 58: 138–152, 1999.
56. **Wong V.** Phosphorylation of occludin correlates with occludin localization and function at the tight junction. *Am J Physiol Cell Physiol* 273: C1859–C1867, 1997.
57. **Zaharchuk G, Mandeville JB, Bogdanov AA Jr, Weissleder R, Rosen BR, and Marota JJ.** Cerebrovascular dynamics of autoregulation and hypoperfusion. An MRI study of CBF and changes in total and microvascular cerebral blood volume during hemorrhagic hypotension. *Stroke* 30: 2197–2205, 1999.
58. **Zlokovic BV, Banks WA, el Kadi H, Erchegyi J, Mackic JB, McComb JG, and Kastin AJ.** Transport, uptake, and metabolism of blood-borne vasopressin by the blood-brain barrier. *Brain Res* 590: 213–218, 1992.
59. **Zlokovic BV, Begley DJ, Djuricic BM, and Mitrovic DM.** Measurement of solute transport across the blood-brain barrier in the perfused guinea pig brain: method and application to *N*-methyl-alpha-aminoisobutyric acid. *J Neurochem* 46: 1444–1451, 1986.